Optics Letters

Recovery of a highly reflective Bragg grating in DPDS-doped polymer optical fiber by thermal annealing

Xuehao Hu,[1] Ning Xu,[2] Xin Cheng,[3] Linyao Tan,[2] Hwa-Yaw Tam,[3] Rui Min,[4] Hang Qu,[2,*] and Christophe Caucheteur[1]

[1]Department of Electromagnetism and Telecommunication, University of Mons, Boulevard Dolez 31, 7000 Mons, Belgium
[2]Research Center for Advanced Optics and Photoelectronics, Department of Physics, College of Science, Shantou University, Shantou, Guangdong 515063, China
[3]Photonics Research Centre, Department of Electrical Engineering, The Hong Kong Polytechnic University, Kowloon, Hong Kong SAR, China
[4]Center for Cognition and Neuroergonomics, State Key Laboratory of Cognitive Neuroscience and Learning, Beijing Normal University, Zhuhai, Guangdong 519087, China
*haqux@stu.edu.cn

Received 1 March 2023; revised 5 April 2023; accepted 5 April 2023; posted 7 April 2023; published 3 May 2023

We report fiber Bragg grating manufacturing in poly(methyl methacrylate) (PMMA)-based polymer optical fibers (POFs) with a diphenyl disulfide (DPDS)-doped core by means of a 266 nm pulsed laser and the phase mask technique. Gratings were inscribed with different pulse energies ranging from 2.2 mJ to 2.7 mJ. For the latter, the grating reflectivity reached 91% upon 18-pulse illumination. Though the as-fabricated gratings decayed, they were recovered by post-annealing at 80°C for 1 day, after which they showed an even higher reflectivity of up to 98%. This methodology for the fabrication of highly reflective gratings could be applied for the production of high-quality tilted fiber Bragg gratings (TFBGs) in POFs for biochemical applications.

https://doi.org/10.1364/OL.487779

Polymer optical fibers (POFs) not only have the same merits as silica optical fibers, such as immunity to electromagnetic interference and a light weight, but also feature extra advantages, including smaller Young's moduli, larger elongation, greater thermo-optic coefficients, and better biocompatibility [1–3]. Since the first successful inscription of a fiber Bragg grating (FBG) in step-index POFs in 1999 [4], FBG inscription has been comprehensively studied in POFs based on different materials, such as poly(methyl methacrylate) (PMMA) [4], cyclic olefin copolymers (TOPAS) [5], cyclic transparent amorphous fluoropolymers (CYTOP) [6], the cyclic-olefin polymer ZEONEX [7,8], and polycarbonate (PC) [9], by either the phase mask or the point-by-point (PbP) direct writing technique [10]. Among different POF materials, PMMA remains the most popular one. In addition, the phase mask technique remains favored for the mass production of FBGs.

In 2002, Liu *et al*. manufactured a grating with a high reflectivity of ~99.8% in a benzyl methacrylate (BzMA)-based POF using a 325 nm laser. However, this inscription process was relatively time consuming (~85 minutes) [11,12]. In 2005, Dobb *et al*. presented the first FBGs in pure PMMA microstructured POFs (mPOFs) obtained using a 325 nm laser [13]. With the development of FBG inscription in PMMA-based POFs, attempts were made to improve the inscription efficiency by doping the core with highly photosensitive materials, including *trans*-4-stilbenemethanol (TS) [14,15], benzyl dimethyl ketal (BDK) [16], and diphenyl disulfide (DPDS) [17,18]. In 2014, a 6-mm-long FBG with a reflectivity of 97% was obtained within 40 minutes in TS-doped POF using a 325 nm laser [19]. In 2021, a 4-mm-long FBG with a reflectivity of 92.7% was obtained in BDK-doped POF via 22-laser-pulse (266 nm) illumination [20].

Additionally, post-annealing after grating inscription is helpful for the recovery of an FBG inscribed in ultra-short time. For example, the reflected band of a 6-mm-long grating inscribed in 1 s in TS-doped POF using a 325 nm CW (continuous wave) He-Cd laser decayed to noise level after 7 days. However, after post-annealing at 80°C for 2 days, the reflectivity of the grating increased by more than 10 dB [21]. For a grating inscribed in BDK-doped POF by a single 266 nm pulse, the grating reflectivity decreased from 97.1% to ~0 within 1 day after inscription, but with post-annealing at 80°C for 1 day, the reflectivity of the grating was re-stabilized at 78.3% [20]. For gratings inscribed in 7 ms, 0.2 s, 0.3 s, and 10 s using a 325 nm CW He-Cd laser in DPDS-doped POF, the reflected peak power gradually increased after inscription [17]. The post-annealing process also substantially diminishes the stabilization time. For example, the stabilization time of the grating inscribed in 0.2 s was reduced from ~250 days at room temperature to ~2 hours by annealing at 60°C [18].

In this work, for the first time to the best of our knowledge, gratings were inscribed in DPDS-doped PMMA POFs using a 266 nm pulsed laser and the phase mask technique. The performance of each of three gratings with different inscription fluences was studied. After inscription, the gratings almost disappeared after one week, but they were regenerated by a thermal annealing treatment at 80°C lasting 1 day, after which they showed even higher reflectivity of up to ~98%. This methodology for the fabrication of highly reflective gratings could

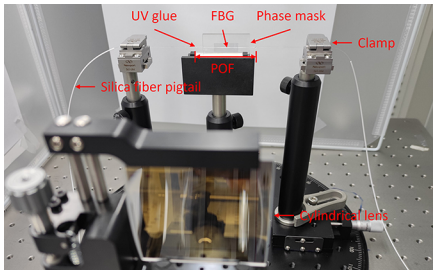

Fig. 1. Experimental setup for grating inscription.

potentially be used for the counterpart of high-quality tilted fiber Bragg gratings (TFBGs) in POFs for biochemical applications.

The POF used here has core and cladding diameters of 5.5 μm and 120 μm, respectively. The dopant DPDS in the fiber core is responsible for increasing both the core refractive index and the photosensitivity [17,18]. The experimental setup for grating inscription was similar to the one reported in our previous work [20], as shown in Fig. 1. A solid-state pulsed laser emitting at 266 nm (DPS-266-Q, Changchun New Industries Optoelectronics Tech. Co., Ltd.) featured a pulse width of ~7 ns, a circular beam spot diameter of ~2.5 mm at the output, and a beam divergence angle of ~1 mrad. The pulse repetition rate was set to 1 Hz in this work. Prior to grating inscription, POFs were pre-annealed at 80°C for 2 days to release the frozen-in stress to ensure better inscription stability [20]. After that, both sides of ~5-cm-long POFs were spliced to silica fiber pigtails using a UV glue (Norland 86 H), allowing the real-time monitoring of the grating spectra during and after the FBG inscription process. The grating spectra were recorded by an FS22SI Industrial BraggMETER Interrogator from HBM FiberSensing S.A., which had a wavelength resolution of 1 pm and a scanning rate of 1 Hz. The phase mask optimized at 266 nm (Phasemask Technology LLC) had a pitch of 1060 nm and was positioned close to and in front of the fiber. A cylindrical lens with a focal length of 15 cm was used to focus the beam onto the fiber core. The grating length was 4 mm and corresponded to the laser beam's dimension along the fiber. Note that although the gratings were inscribed for ~1550 nm in PMMA POFs, they could also be inscribed for ~850 nm or visible wavelengths with much lower transmission loss by using phase masks with the proper pitch [22].

Figure 2 depicts the transmitted amplitude spectra recorded at the end of the photo-inscription process for three FBGs inscribed using different pulse energies and pulse quantities (2.2 mJ, 113 pulses for FBG 1, 2.5 mJ, 40 pulses for FBG 2, and 2.7 mJ, 21 pulses for FBG 3). The measured depths of the FBG resonances

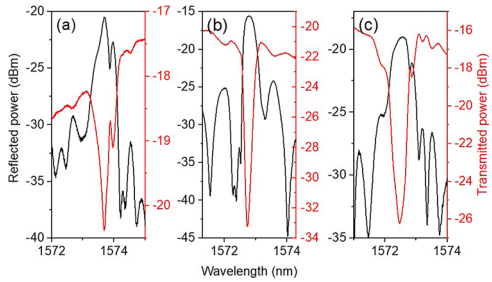

Fig. 2. Reflected and transmitted amplitude spectra of the FBGs inscribed using different pulse energies and pulse numbers: (a) 2.2 mJ, 113 pulses for FBG 1; (b) 2.5 mJ, 40 pulses for FBG 2; (c) 2.7 mJ, 21 pulses for FBG 3.

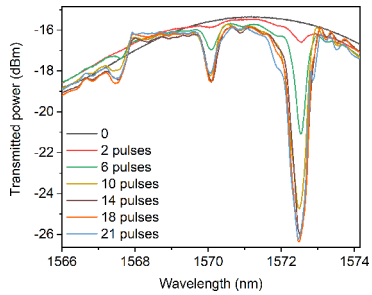

Fig. 3. Evolution of the transmitted amplitude spectrum of FBG 3 during the photo-inscription process.

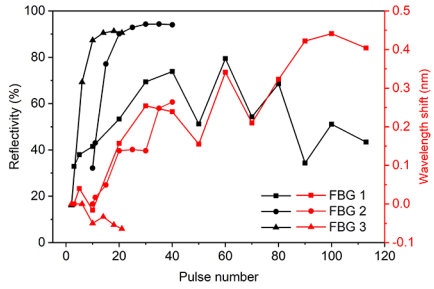

Fig. 4. FBG growth dynamics in reflectivity computed from insertion loss measurements and Bragg wavelength shifts in the FBG transmitted amplitude spectra.

are 2.5 dB, 12.2 dB, and 10.2 dB, corresponding to a reflectivity of 43%, 94%, and 90%, respectively. These observations require a closer look at the grating formation mechanism, as reported hereafter.

Figure 3 shows the dynamic growth of FBG 3 measured from its transmitted amplitude spectrum. During the writing process, the FBG rejection band grows rapidly and becomes saturated after 14 pulses. Note that the presence of three grating peaks is due to the few-mode guiding property of this fiber. However, as the peaks of the two higher-order modes besides the fundamental mode are relatively small, only the fundamental mode is discussed and investigated in this work. The fiber out-of-band insertion loss induced by photo-irradiation increases during the grating inscription process and reaches up to ~1 dB.

Figure 4 depicts the reflectivity evolution of the three FBGs. For FBG 1, it grows until 60 pulses of irradiation have occurred to a reflectivity of 79% and then gets saturated. The saturation could be attributed to the instability of refractive modifications. For FBG 2, the grating reflectivity reached a maximum of 94% with 35 pulses of irradiation. For FBG 3, the reflectivity increased to 91% with 18 pulses of irradiation. It is found that the pulse energy is approximately proportional to the grating inscription efficiency.

In order to provide better insight for understanding the FBG growth process in such fibers when using the 266 nm pulsed laser, the FBG wavelength shift evolution during the grating fabrication process is also shown in Fig. 4. For FBG 1 and FBG 2, a wavelength redshift of 404 pm and 264 nm, respectively, is observed, while for FBG 3, the grating wavelength undergoes a blueshift of 64 pm. This Bragg wavelength shift is related to the variations in the effective refractive index of the fiber mode [23]. It is worth mentioning that, compared to silica fibers, polymer fibers feature inherent characteristics such as higher absorption

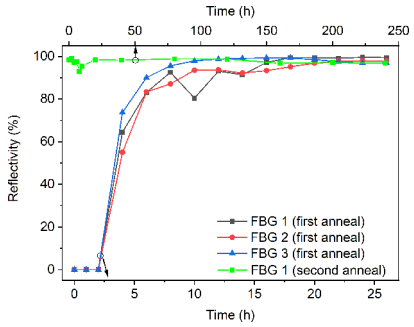

Fig. 5. Reflectivity evolutions of FBGs 1–3 during the annealing process at 80°C.

of UV light and higher thermal swelling due to laser heating, such that a smaller pulse energy is preferable for FBG inscription in POFs.

After FBG inscription, all the gratings had almost disappeared after one week at room temperature, in a similar way to the cases reported in Refs. [20,21]. To solve this problem, post-irradiation thermal annealing at 80°C for 26 hours (2 h with a linear rising edge and 24 h at constant temperature) was conducted to recover the strength of the FBGs. The FBGs showed a similar dynamic evolution of the reflectivity during the whole annealing process, as shown in Fig. 5. From 2 h, the grating reflectivities start to grow, and then they gradually reach ~90% at 10 h. Finally, at 26 h, ~98% reflectivity is obtained. Forty days after the initial annealing, we carried out another annealing process for FBG 1 with a much longer duration of 240 h (2 h with a linear rising edge and 238 h at constant temperature) at 80°C, during which FBG 1 shows a stable reflectivity of ~97%, as shown in Fig. 5.

The Bragg wavelength shifts of these FBGs during the annealing process are shown in Fig. 6. These blueshifts may have been caused by the release of the frozen-in stress generated during the fiber drawing process [21] and the negative thermo-optic coefficient of PMMA [24]. Though the wavelength shifts did not stabilize during the annealing process, excellent thermal stability of the fabricated FBGs in the same fiber in the range of 20–50°C was proved in our previous work [17]. Note that though the biocompatibility of DPDS has not been proved, it is used as a dopant in the fiber core and is thus completely isolated. For practical applications, it would not produce any harmful effects

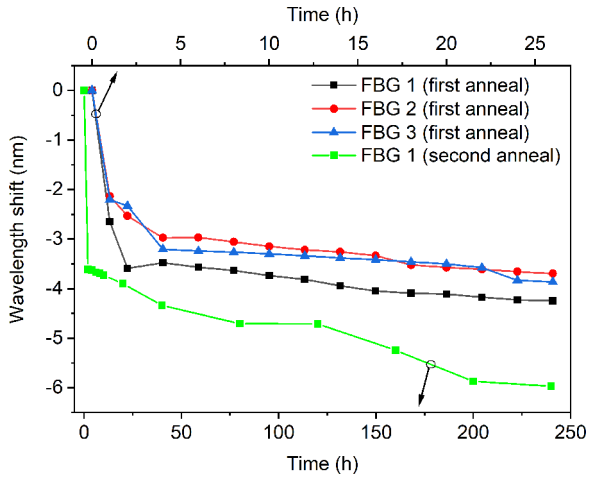

Fig. 6. Bragg wavelength shifts of FBGs 1–3 during the annealing process at 80°C.

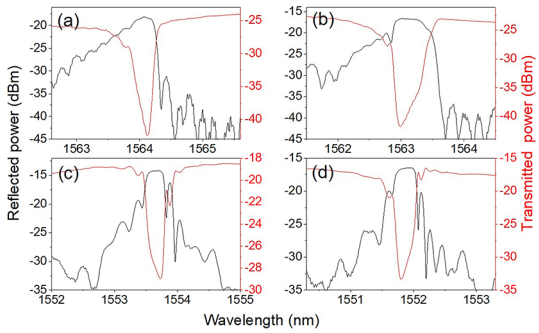

Fig. 7. Reflected and transmitted amplitude spectra of (a) FBG 1 (40 days after the first annealing), (b) FBG 1 (112 days after the second annealing), (c) FBG 2 (80 days after annealing), and (d) FBG 3 (80 days after annealing).

on the application environment. Thus, the FBGs qualify for biomedical applications and could potentially be applied for *in vivo* sensing. After the annealing process, FBG 1–3 were kept at room temperature. All the reflected and transmitted spectra are shown in Fig. 7, which shows reflectivities of 98% for FBG 1 (40 days after the first annealing), 99% for FBG 1 (112 days after the second annealing), 90% for FBG 2 (80 days after annealing), and 98% for FBG 3 (80 days after annealing).

It has been proved that the dopant DPDS plays a significant role in the core refractive index modulation in the DPDS-doped PMMA POF. Using a 325 nm CW He-Cd laser and the phase mask technique, a grating was obtained within 7 ms and showed a signal-to-noise ratio of 7 dB in reflection. Without using the phase mask technique, after 4 s of UV irradiation at 325 nm, a positive refractive index variation of $\sim 5 \times 10^{-4}$ was measured [17]. Thus, in this work, we attribute the efficient FBG inscription to the presence of the dopant. The mechanism for the refractive index change of the core material could be explained as follows: (1) PMMA starts to degrade upon UV irradiation below ~300 nm [25]; (2) the S–S bond of DPDS can be broken under UV irradiation, leading to the instant generation of two sulfenyl radicals [17,26] ~2 μs after UV absorption [27]; (3) the sulfenyl radicals can attach to photodegraded sites on the PMMA chain through the sulfur atom (the most likely routes are the cleavage of OCH_3 from the side chain or total side-chain scission followed by replacement with the sulfenyl radicals [17]); and (4) the addition of aromatic rings and sulfur atoms is known to increase the refractive index of DPDS-doped PMMA material [28].

In our work, we have found several interesting phenomena, which can be summarized as follows. Generally, after inscription, the grating reflectivity tends to decrease, but after post-annealing, the grating recovers a stable reflectivity. We believe that these individual phenomena are related to the strength of the refractive index modulation generated in the fiber core [23]. To provide some insight to explain these phenomena, we have analyzed the literature on this subject. During the FBG inscription process, we assume that the laser pulses periodically heat the fiber core and thus promote the motion of polymer chain segments, generating sufficient free volume to facilitate the partial or total replacement of the side chain with sulfenyl radicals [15]. The contradictory effective refractive index changes of the fiber corresponding to central Bragg wavelength shifts (redshifts for FBG 1 and 2; a blueshift for FBG 3) could arise from the competition between the chemical

Table 1. Comparison of Highly Reflective FBGs Inscribed in Step-Index PMMA-Based POFs

Core Dopant	Laser	Time or Pulse Quantity	Post-Annealing	Final Reflectivity (%)	Ref.
BzMA	325 nm pulsed	85 min 10 Hz	No	99.8	[11,12]
TS	325 nm CW	40 min	No	97	[19]
BDK	266 nm pulsed	22 pulses 0.25 Hz	No	92.7	[20]
BDK	266 nm pulsed	1 pulse	Yes	78.3	[20]
DPDS	266 nm pulsed	21 pulses 1 Hz	Yes	98	This work

reaction (resulting in an increase in the refractive index) and heat accumulation (resulting in a decrease in the refractive index due to a negative thermo-optic coefficient [24]). The decrease in FBG reflectivity can be attributed to the instability of the side-chain replacement in the polymer matrix; the reverse reaction may also occur, which would reduce the strength of the refractive index modulation. Then, the post-annealing at 80°C, which is above the melting point of DPDS (62°C) [29], may accelerate the movement of sulfenyl radicals to substitute the side chain of PMMA. The stability of the grating could be attributed to the completion of the chemical reactions.

Finally, the high-quality gratings achieved in this work are compared with counterparts obtained in previous works, as shown in Table 1. For the FBG in the BzMA-doped fiber, though a very high reflectivity of 99.8% was achieved, it took 85 minutes to inscribe [11,12]. For the BDK-doped fiber, a FBG was inscribed by a single pulse; however, the reflectivity was only 78.3% [20]. In terms of this work, FBG 3 inscribed with 21 pulses presented a reflectivity of 98% after post-annealing, which represents the best balance between inscription time and grating reflectivity. This combination could facilitate the mass production of high-quality FBGs in POFs.

In this work, we have studied the grating inscription and spectral evolution as a function of time in pre-annealed DPDS-doped step-index PMMA POFs. The obtained performance is related to the pulse energy, the core material, and the post-annealing treatment. These results can be explained by the movement of sulfenyl radicals homolyzed from DPDS under UV irradiation. This work has shown that both grating reflectivity and stability can be improved by post-irradiation thermal annealing at 80°C. The proposed route paves the way to the production of high-quality gratings in POFs, with a high potential for producing specialty gratings, such as tilted ones that are very useful in biochemical applications.

Funding. Special Projects in Key Fields of Colleges and Universities in Guangdong Province (2020ZDZX3037); Science and Technology Department of Guangdong Province (2022A1515012571); Fonds De La Recherche Scientifique - FNRS.

Acknowledgments. Funding from Fonds De La Recherche Scientifique (F. R. S. - FNRS) is under the Postdoctoral Researcher grant (Chargé de Recherches) of Xuehao Hu and the Senior Research Associate Position of Christophe Caucheteur.

Disclosures. The authors declare no conflicts of interest.

Data availability. Data underlying the results presented in this paper are not publicly available at this time but may be obtained from the authors upon reasonable request.

REFERENCES

1. D. J. Webb, Meas. Sci. Technol. **26**, 092004 (2015).
2. Y. Wang, Y. Huang, H. Bai, G. Wang, X. Hu, S. Kumar, and R. Min, Biosensors **11**, 472 (2021).
3. R. He, C. Teng, S. Kumar, C. Marques, and R. Min, IEEE Sens. J. **22**, 1081 (2022).
4. Z. Xiong, G. D. Peng, B. Wu, and P. L. Chu, IEEE Photonics Technol. Lett. **11**, 352 (1999).
5. I. P. Johnson, W. Yuan, A. Stefani, K. Nielsen, H. K. Rasmussen, L. Khan, D. J. Webb, K. Kalli, and O. Bang, Electron. Lett. **47**, 271 (2011).
6. A. Theodosiou and K. Kalli, Opt. Fiber Technol. **54**, 102079 (2020).
7. G. Woyessa, H. K. Rasmussen, and O. Bang, Opt. Fiber Technol. **57**, 102231 (2020).
8. X. Cheng, D. S. Gunawardena, C.-F. J. Pun, J. Bonefacino, and H.-Y. Tam, Opt. Express **28**, 33573 (2020).
9. G. Woyessa, A. Fasano, C. Markos, H. K. Rasmussen, and O. Bang, IEEE Photonics Technol. Lett. **29**, 575 (2017).
10. C. Broadway, R. Min, A. G. Leal-Junior, C. Marques, and C. Caucheteur, J. Lightwave Technol. **37**, 2605 (2019).
11. H. Y. Liu, G. D. Peng, and P. L. Chu, IEEE Photonics Technol. Lett. **14**, 935 (2002).
12. H. Y. Liu, H. B. Liu, G. D. Peng, and P. L. Chu, Opt. Commun. **220**, 337 (2003).
13. H. Dobb, D. J. Webb, K. Kalli, A. Argyros, M. C. J. Large, and M. A. V. Eijkelenborg, Opt. Lett. **30**, 3296 (2005).
14. J. M. Yu, X. M. Tao, and H. Y. Tam, Opt. Lett. **29**, 156 (2004).
15. J. M. Yu, X. M. Tao, and H. Y. Tam, Opt. Commun. **265**, 132 (2006).
16. Y. Luo, Q. Zhang, H. Liu, and G. D. Peng, Opt. Lett. **35**, 751 (2010).
17. J. Bonefacino, H.-Y. Tam, T. S. Glen, X. Cheng, C.-F. J. Pun, J. Wang, P.-H. Lee, M.-L. V. Tse, and S. T. Boles, Light: Sci. Appl. **7**, 17161 (2017).
18. J. Bonefacino, X. Cheng, C.-F. J. Pun, S. T. Boles, and H.-Y. Tam, Opt. Express **28**, 1158 (2020).
19. X. Hu, C.-F. J. Pun, H.-Y. Tam, P. Mégret, and C. Caucheteur, Opt. Express **22**, 18807 (2014).
20. X. Hu, X. Yue, X. Cheng, S. Gao, R. Min, H. Wang, H. Qu, and H. Y. Tam, Opt. Lett. **46**, 2864 (2021).
21. X. Hu, D. Kinet, P. Mégret, and C. Caucheteur, Opt. Lett. **41**, 2930 (2016).
22. A. Stefani, W. Yuan, C. Markos, and O. Bang, IEEE Photonics Technol. Lett. **23**, 660 (2011).
23. T. Erdogan, J. Lightwave Technol. **15**, 1277 (1997).
24. G. Khanarian, Opt. Eng. **40**, 1024 (2001).
25. S. D. Alshehry and I. M. I. Ismail, Orient. J. Chem. **24**, 35 (2008).
26. G. P. Russell, J. Phys. Chem. **79**, 1353 (1975).
27. R. M. Abaskharona and F. Gai, Phys. Chem. Chem. Phys. **18**, 9602 (2016).
28. T. Higashihara and M. Ueda, Macromolecules **48**, 1915 (2015).
29. https://commonchemistry.cas.org/detail?cas_rn=882-33-7.